Mano, Ed., Elsevier, Amsterdam, 1975, p 169.

(15) R. Ditchfield, D. P. Miller, and J. A. Pople, *J. Chem. Phys.*, **54**, 4186 (1971).

(16) M. Kondo, I. Ando, R. Chûjô, and A. Nishioka, *J. Magn. Reson.*, **24**, 315 (1976).

(17) I. Ando and T. Asakura, *Annu. Rept. NMR Spectrosc.*, **10A**, 81 (1980).

(18) K. A. K. Ebraheem and G. A. Webb, *Prog. Nucl. Magn. Reson. Spectrosc.* **11**, 149 (1977).

(19) (a) I. Shavitt and M. Karplus, *J. Chem. Phys.*, **43**, 398 (1965); (b) C. W. Kern and M. Karplus, *ibid.*, **43**, 415 (1965).

(20) F. A. Momany, R. F. McGuire, J. F. Yan, and H. A. Scheraga, *J. Phys. Chem.*, **75**, 2286 (1971).

(21) S. Arnott and A. L. Wonacott, *J. Mol. Biol.*, **21**, 371 (1966).

(22) S. Arnott, S. D. Dover, and A. Elliot, *J. Mol. Biol.*, **30**, 201 (1967).

(23) K. Itoh, T. Nakahara, T. Shimanouchi, M. Oya, K. Uno, and Y. Iwakura, *Biopolymers*, **6**, 1759 (1968).

(24) Recently, we have observed that the C_α and carbonyl ^{13}C chemical shifts of the left-handed α-helical poly(β-benzyl-L-aspartate) $(Asp(OBzl)_n)$, cast from chloroform solution and dried quickly, are very close to those of the β-sheet form, although the C_β signal is identical with that of the right-handed α-helical $(Asp(OBzl)_n)$. (H. Saito, R. Tabeta, I. Ando, T. Ozaki, and A. Shoji, *Chem. Lett.*, 1437 (1983).) This observation strongly supports our present assignment of the peaks i. As to the assignment of the peak i in the C_β carbon, one of the reviewers raised a question as follows. When a D-alanine adopts the α_R helix its C_β carbon and carbonyl oxygen atoms are eclipsed, or cis. This overlapped arrangement of C_β is removed to L-alanine in the α_R-helix. It is pointed out in ref 7 that this eclipsed arrangement is highly shielding and would be expected to result in the D-alanine C_β resonance appearing upfield from the C_β resonance in L-alanine (α_R-helix). This view, however, is incorrect as viewed from the present experimental finding as well as that of $(Asp(OBzl)_n)$. It is also emphasized that the variation of ^{13}C chemical shifts, similar to that of $(Ala)_n$, is well reproduced by a theoretical calculation (I. Ando et al., manuscript in preparation).

(25) F. A. Bovey in "Macromolecules, An Introduction to Polymer Science", F. A. Bovey and F. H. Winslow, Eds., Academic Press, New York, 1979, Chapter 8.

Isotactic Polymerization of C-3 Branched α-Olefins: Conformation of the Monomer[1]

A. Zambelli,* P. Ammendola, and A. J. Sivak[2]

Istituto Chimico dell'Università di Napoli, 80134 Naples, Italy. *Received May 31, 1983*

ABSTRACT: The rate constants of the initiation on metal–methyl bonds for isotactic polymerization of 3-methyl-1-pentene (3MP1), 3-methyl-1-butene (3MB1), and 3-ethyl-1-pentene (3EP1) have been compared to each other. Their relative values are accounted for by assuming that the monomers react with a possibly distorted H-skew or H-skew′ conformation.

1. Introduction

In a previous paper it was pointed out that insertion of 3-methyl-1-pentene (3MP1) into the reactive metal–carbon bond of the active sites of Ziegler–Natta isotactic-specific catalysts is diastereoselective. It was actually observed that the *R′,R* and *S′,S* faces of the racemic monomer are twice as reactive as the *S′,R* and *R′,S* faces (Figure 1) both in the enantioselective chain propagation steps and in the nonenantioselective initiation on $Mt–CH_3$ bonds.[3,4]

If one considers the most favored solution-state conformation of the olefin (H-syn)[5–8] (see Figure 2), it turns out that the more reactive faces of 3MP1 (*R′,R* and *S′,S*) also appear to be the most hindered.

On the other hand, it is quite possible that the monomer is forced to achieve a different conformation in order to approach the reactive metal–carbon bond of the active site with a minimum of nonbonded interactions.

In this paper the reactivity of the diastereotopic faces of 3MP1 in the initiation on $Mt–CH_3$ bonds is compared with the reactivity of the enantiotopic faces of 3-methyl-1-butene (3MB1) and 3-ethyl-1-pentene (3EP1). Some information concerning the conformation of the monomer in the active state is inferred.

2. Experimental Section

Reagents. 3MB1 was prepared according to the literature.[9] (*RS*)-3MP1 and 3EP1 were commercial products. The purity of the monomers was checked by GLC (>98%). The monomers and the polymerization diluent (pentane) were distilled under vacuum in the presence of a small amount of $Al(n\text{-}C_4H_9)_3$ just before polymerization. ^{13}C-enriched (34%) $Al(CH_3)_3$ and $Zn(CH_3)_2$ were prepared according to ref 10. δ-$TiCl_3$ was prepared according to the literature[11] (elemental analysis: Ti, 20.18; Al, 7.45; Cl, 69.60).

Copolymerization of 3MB1 and (*RS*)-3MP1. Five milliliters of anhydrous pentane, 4.9×10^{-3} mol of δ-$TiCl_3$, 1.2×10^{-3} mol of $Al(^{13}CH_3)_3$, and 2.9×10^{-3} mol of $Zn(^{13}CH_3)_2$ were introduced under nitrogen into a 60-mL reactor provided with a magnetic stirring bar and cooled to −78 °C. The reactor was then cooled with liquid nitrogen and evacuated with a diffusion pump. Next, 1.2×10^{-1} mol of (*RS*)-3MP1 and 2.6×10^{-2} mol of 3MB1 were condensed into the reactor through a vacuum line. The reactor was transferred into a thermostated bath. After 5 h of stirring at 50 °C the polymerization was stopped by injecting 5 mL of 2-ethylhexanol into the reactor. Polymer yield was 0.65 g.

Copolymerization of 3EP1 and (*RS*)-3MP1. The copolymerization was performed as above, with 5 mL of pentane, 6×10^{-3} mol of δ-$TiCl_3$, 1.3×10^{-3} mol of $Al(^{13}CH_3)_3$, 3.1×10^{-3} mol of $Zn(^{13}CH_3)_2$, 6.2×10^{-2} mol of (*RS*)-3MP1, and 9.2×10^{-2} mol of 3EP1. Polymerization time was 20 h; yield was 0.4 g.

Fractionation. The copolymers were fractionated by subsequent exhaustive extractions with boiling diethyl ether and toluene.[12] The results are reported in Table I.

^{13}C NMR Analysis. Proton-noise-decoupled ^{13}C NMR analysis of the samples dissolved in 1,2,4-trichlorobenzene containing 20% tetrachloroethane-*1,2*-d_2 for field-frequency stabilization and HMDS as an internal standard was carried out at 130 °C in the PFT mode on a Varian XL-200 spectrometer operating at 50.309 MHz. Pulse width was 4.7 μs. The fractions insoluble in boiling toluene were thermally degraded as described in ref 3.

X-ray Analysis. X-ray spectra of unoriented samples were obtained with a Philips APD spectrometer using Cu Kα radiation. Both the toluene-soluble fractions and the toluene-insoluble fractions were found to have nearly the same degree of crystallinity.

3. Results

(*RS*)-3MP1 has been copolymerized with 3MB1 or 3EP1 in the presence of the isotactic-specific catalytic system

0024-9297/84/2217-0461$01.50/0

Table I
Fractionation Results and Diastereoselectivity Data

	(*RS*)-3MP1-3MB1				(*RS*)-3MP1-3EP1			
fraction	*E*[a]	*B*[a]	*T*[a]	wt %	*E*[a]	*P*[a]	*T*[a]	wt %
diethyl ether soluble	0.48	0.26	0.26	14	0.51	0.23	0.26	9
ether insoluble								
toluene soluble	0.48	0.26	0.26	9	0.51	0.23	0.26	22
toluene insoluble[b]	0.48	0.26	0.26	77	0.51	0.23	0.26	69

[a] Normalized intensities of the E, T, B, and P resonances (see Figures 3 and 4). [b] The toluene-insoluble fractions were observed after thermal degradation. As reported in ref 3, epimerization of the end groups should be negligible.

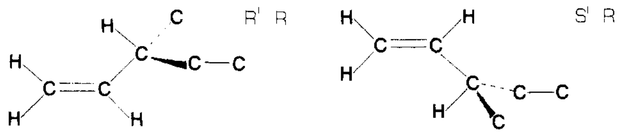

Figure 1. Diastereotopic faces of (-)-(*R*)-3MP1.

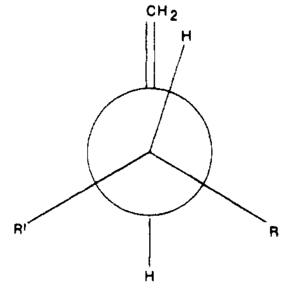

Figure 2. Newman projection of the H-syn conformation of an α-olefin branched on C-3.

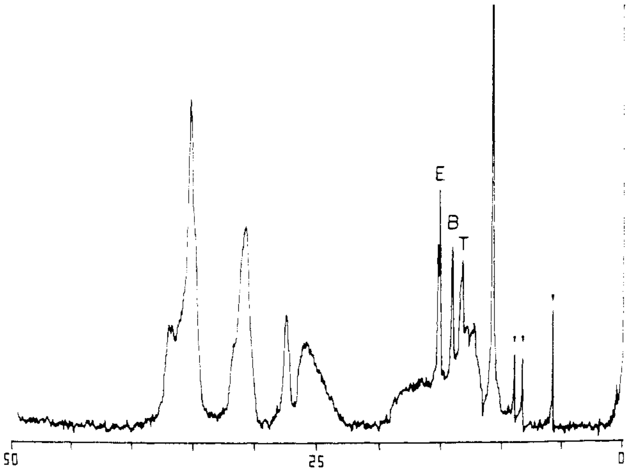

Figure 3. ^{13}C NMR spectrum of the diethyl ether insoluble–toluene soluble fraction of poly[(*RS*)-3MP1–3MB1]. HMDS scale. The peaks marked by triangles arise from folding of the solvent resonances.

δ-$TiCl_3$–$Al(^{13}CH_3)_3$–$Zn(^{13}CH_3)_2$ at 50 °C. ^{13}C-enriched organometallic cocatalysts have been used in order to be able to detect by ^{13}C NMR the "right" end groups[3] of the polymer, which arise from the insertion of the first monomer into the Mt–$^{13}CH_3$ bonds, as shown below.

$$Mt\text{-}^{13}CH_3 + CH_2{=}CHR \rightarrow Mt\text{-}CH_2\text{-}CH(R)\text{-}^{13}CH_3$$

The copolymers have been fractionated by exhaustive sequential extraction with boiling diethyl ether and boiling toluene. All fractions, including the ones insoluble in boiling toluene, were analyzed by ^{13}C NMR. The spectra of the toluene-soluble fractions of the poly[(*RS*)-3MP1–3MB1] and the poly[(*RS*)-3MP1–3EP1] are reported, as an example, in Figures 3 and 4. The resonances most relevant to this paper are those centered at 13.4 ppm (T) and 15.2 ppm (E) in both spectra, the one centered at 14.2 ppm (B) in the spectrum of poly[(*RS*)-3MP1–3MB1], and the one centered at 14.5 ppm (P) in the spectrum of poly[(*RS*)-3MP1–3EP1]. The resonances centered at 13.4 and 15.2 ppm have previously been assigned[3] to the enriched methyl carbons of the 2,3-dimethylpentyl-2'-^{13}C groups arising from the insertion of (*RS*)-3MP1. The different chemical shifts are a consequence of the two possible diastereomeric placements (*R'*,*S* and *S'*,*R*, or E; *S'*,*S* and *R'*,*R*, or T)[3,4] of the 2'- and 3'-methyl groups (Figure 5). Notice that, as reported in ref 3, the resonance of the E methyls, at 15.2 ppm, involves attack on the *R'*,*R* and *S'*,*S* faces of the monomer, while the resonance of the T methyls, at 13.4 ppm, involves attack on the *S'*,*R* and *R'*,*S* faces (Figure 6). The resonance centered at 14.2 ppm in Figure 3 and that at 14.5 ppm in Figure 4 can be as-

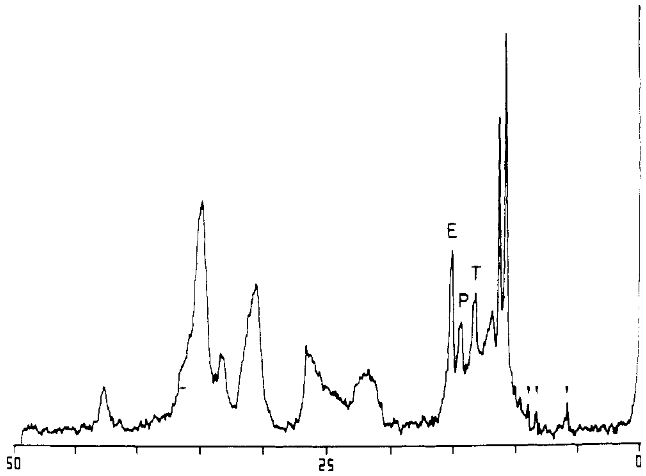

Figure 4. ^{13}C NMR spectrum of the diethyl ether insoluble–toluene soluble fraction of poly[(*RS*)-3MP1–3EP1]. HMDS scale. The peaks marked by triangles arise from folding of the solvent resonances.

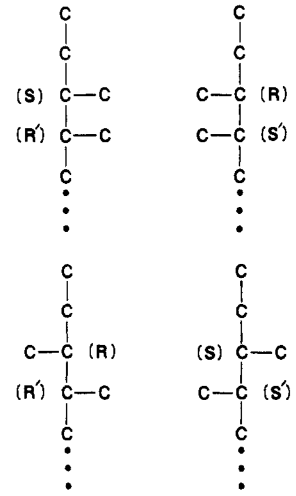

Figure 5. Fischer projections of the 2,3-dimethylpentyl end groups.

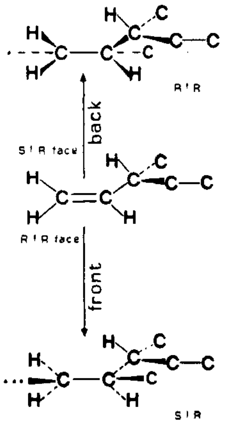

Figure 6. Diastereoisomeric end groups *S′,R* and *R′,R*, arising from attack on the front face (*R′,R*) or the back face (*S′,R*) of (−)-(*R*)-3MP1.

signed, by comparison with similarly enriched homopolymers as well as on the basis of the Lindemann and Adams chemical shift correlations,[13] to the enriched methyls of the 2,3-dimethylbutyl-2′-^{13}C (B) and 3-ethyl-2-methylpentyl-2′-^{13}C (P) groups, respectively. Of course, they arise from the insertion of 3MB1 and 3EP1 into Mt–$^{13}CH_3$.

The other ^{13}C resonances observed in the spectra considered arise from the inner carbons of the macromolecule and are not directly relevant to this paper. Nonetheless, it is worthwhile to say that they are broad just because of the presence of chemically and sterically different substituents. In fact, considering the results reported in ref 3 concerning poly[(*RS*)-3MP1], it is expected that at least the fractions insoluble in diethyl ether are highly coisotactic. Some copolymer is soluble in toluene mainly because of low molecular weight. As a matter of fact dimethylzinc is known[3,14] to be a very efficient chain-transfer agent in Ziegler–Natta polymerization of olefins. A stereoregular structure for the substituted carbons of the copolymer backbone is also suggested by the fact that the copolymer fractions under consideration appear crystalline by X-ray analysis.

The normalized intensities for the resonances of the enriched methyls considered are reported in Table I for all the fractions of the two copolymers. Notice that the normalized intensities are almost the same for all the fractions of each copolymer.

Both copolymers were prepared with very low conversions. The compositions of the feeds are reported in the Experimental Section.

4. Discussion

Initiation Rate Constants. The ^{13}C-enriched end groups considered thus far arise from the initiation steps shown in Scheme I for the (*RS*)-3MP1–3MB1 copolymer. Notice that since the insertion of α-olefins into the Mt–$^{13}CH_3$ bonds of the active site is not enantioselective,[10] the asymmetric structure of the active sites is neglected. Instead the steps leading to enantiomorphous end groups are considered separately. Of course, by symmetry

$$k_{(R')\text{-B}} = k_{(S')\text{-B}}; \qquad k_{R'R} = k_{S'S}; \qquad k_{S'R} = k_{R'S}$$

Likewise

$$[(R')\text{-2,3DMB}] = [(S')\text{-2,3DMB}]$$

and since racemic 3MP1 was used

$$[(R',R)\text{-2,3DMP}] = [(S',S)\text{-2,3DMP}]$$
$$[(S',R)\text{-2,3DMP}] = [(R',S)\text{-2,3DMP}]$$

Scheme I[a]

$$\left.\begin{array}{l}\text{Mt—CH}_3 + \text{3MB1} \xrightarrow[k_{(R')\text{-B}}]{} (R')\text{-2,3DMB} \\ \text{Mt—CH}_3 + \text{3MB1} \xrightarrow[k_{(S')\text{-B}}]{} (S')\text{-2,3DMB}\end{array}\right. \qquad \text{(B)}$$

$$\left.\begin{array}{l}\text{Mt—CH}_3 + (R)\text{-3MP1} \xrightarrow[k_{R'R}]{} (R',R)\text{-2,3DMP} \\ \text{Mt—CH}_3 + (S)\text{-3MP1} \xrightarrow[k_{S'S}]{} (S',S)\text{-2,3DMP}\end{array}\right. \qquad \text{(T)}$$

$$\left.\begin{array}{l}\text{Mt—CH}_3 + (R)\text{-3MP1} \xrightarrow[k_{S'R}]{} (S',R)\text{-2,3DMP} \\ \text{Mt—CH}_3 + (S)\text{-3MP1} \xrightarrow[k_{R'S}]{} (R',S)\text{-2,3DMP}\end{array}\right. \qquad \text{(E)}$$

[a] 2,3DMB = 2,3-dimethylbutyl; 2,3DMP = 2,3-dimethylpentyl.

Assuming that the molar fraction of the end groups of the copolymers considered so far is proportional to the rate of the insertion steps reported in Scheme I, the intensities of the corresponding resonances (E, T, and B in Figure 3) can be correlated with the monomer feed.

$$E \propto 2k_{S'R}[(R)\text{-3MP1}] = k_{S'R}[(RS)\text{-3MP1}]$$
$$T \propto 2k_{R'R}[(R)\text{-3MP1}] = k_{R'R}[(RS)\text{-3MP1}]$$
$$B \propto 2k_{(R')\text{-B}}[\text{3MB1}]$$

A similar correlation is obviously obtained for the enriched end groups of the 3MP1–3EP1 copolymer. Thus

$$E \propto k_{S'R}[(RS)\text{-3MP1}]$$
$$T \propto k_{R'R}[(RS)\text{-3MP1}]$$
$$P \propto 2k_{(R')\text{-P}}[\text{3EP1}]$$

Assuming, in arbitrary units, that

$$k_{R'R} = 1$$

we have determined that

$$k_{S'R} = 1.9$$

(which is in close agreement with ref 3) and

$$k_{(R')\text{-B}} = 2.3; \qquad k_{(R')\text{-P}} = 0.3$$

Conformation of the Monomer in the Active State. The overall stereochemical mechanism of addition to the double bond in Ziegler–Natta polymerization of α-olefins is of the cis type.[15,16] This fact strongly suggests suprafacial attack by the reactive metal–carbon bond on one face of the monomer. The distribution of the π-electrons of the α-olefins considered here should be essentially the same. As a consequence the relative rate constants of the insertion steps of Scheme I should only be dependent on the shape of the attacked olefin face. In turn, the shape of the face to be attacked depends on the conformation of the substituent group of the olefin. Thus, knowing that $k_{S'R} > k_{R'R}$ and assuming (a) that at the moment of attack the monomer possesses the H-syn conformation (Figure 2) and (b) that the population of the H-syn conformation should increase with increasing steric demand of the substituents on C-3, one might conclude, simply by inspection of Figure 7, that the following relations should exist

$$k_{(R')\text{-P}} > k_{S'R} > k_{R'R} > k_{(R')\text{-B}}$$

This conclusion is not consistent with the experimentally determined values of the *k*'s as reported in the previous section. It is worth noting that during the course of this work we have also observed that neohexene does not react with the Mt–CH_3 of the active sites to any appreciable degree. This suggests that a requirement for a monomer

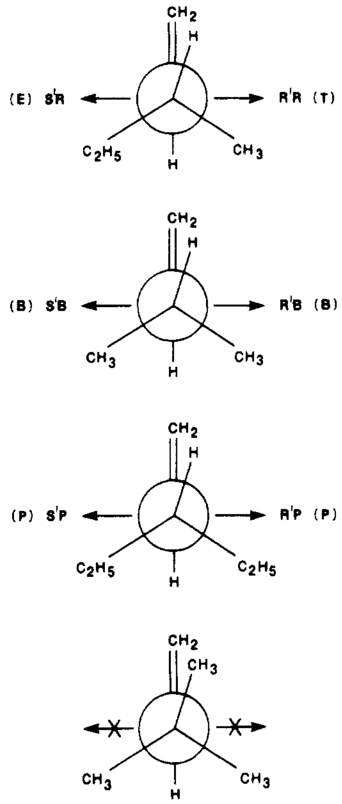

Figure 7. Newman projections of the H-syn conformations of (–)-(*R*)-3MP1, 3MB1, and 3EP1. The configurational notations of the end groups arising from the attack on either face are shown by the arrows. The bottom of the figure shows the CH_3-syn conformation of neohexene.

face to be reactive could be that the conformation of the monomer must be such that no alkyl group protrudes out of the plane of the double bond in the direction of the attack. This requirement is met, for example, in the H-skew and H-skew′ conformations reported in Figure 8. In this case, considering (a) the previous assumption concerning the population of the H-syn conformation and (b) that the H-skew or H-skew′ conformation, which has the bulkier substituent eclipsed with C-1, has the higher energy and hence a lower population, one could foresee, simply upon inspection of Figure 8

$$k_{(R')\text{-B}} > k_{S'R} > k_{R'R} > k_{(R')\text{-P}}$$

These relations among the *k*'s are consistent with the experimental results. More accurate comparison among the *k*'s should involve quantitative conformational analysis and consideration of the nonbonded interactions with the approaching active site and the possibility of consequent conformational deformations. This is beyond the scope of this paper.

5. Conclusion

The diastereoselectivity of the insertion of (*RS*)-3MP1 into Mt–CH_3 bonds in the initiation of Ziegler–Natta isotactic-specific polymerization, as well as the relative reactivity of 3MP1, 3MB1, and 3EP1 in the same reaction, should depend on the steric hindrance of the monomer faces presented to and attacked by the Mt–CH_3. The actual nonbonded interactions in the active state depend on the conformation of the monomer that is about to react and the direction of approach of the Mt–CH_3.

In this paper we have tried to select among the possible conformations of the monomers those which can account for the experimentally observed reaction rates. The conclusion reached is that the more stable conformations of the monomers in solution (those with H-syn)[5–7] are unreactive. The H-skew and H-skew′ conformations seem to account, at least qualitatively, for the relative rates of the diastereomeric attacks on 3MP1 as well as for the relative reactivities of the investigated monomers. This result seems to be distinctive of isotactic polymerization. As a matter of fact, a distorted H-syn conformation of 3MP1 has been observed in coordination compounds,[17,18] and the *S′,R* (*R′,S*) face of 3MP1 has been found the most reactive in Rh-catalyzed hydroformylation[19] to 4-methylhexanal.

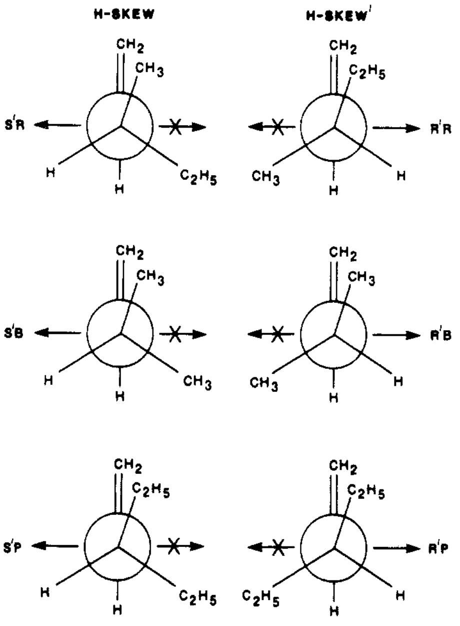

Figure 8. Newman projection of the H-skew and H-skew′ conformations of (–)-(*R*)-3MP1, 3MB1, and 3EP1. The arrows show the configurational notations for the end groups resulting from the allowed attacks.

Registry No. 3-Methyl-1-pentene, 760-20-3; 3-methyl-1-butene, 563-45-1; 3-ethyl-1-pentene, 4038-04-4.

References and Notes

(1) Financial support of the Programma Finalizzato di Chimica Fine e Secondaria of the Italian CNR is gratefully acknowledged.
(2) Gulf Research Center, Pittsburgh, PA.
(3) Zambelli, A.; Ammendola, P.; Sacchi, M. C.; Locatelli, P.; Zannoni, G. *Macromolecules* **1983**, *16*, 341.
(4) The configurations of the end groups are given according to the absolute configuration of C-2 and, eventually, C-3 (Cahn, R. S.; Ingold, C. R.; Prelog, V. *Angew. Chem., Int. Ed. Engl.* **1956**, *5*, 565). However, isotopic substitution is neglected. The configurations of the monomer faces are given according to the configuration of the enantiotopic C-2 (Paiaro, G.; Panunzi, A. *J. Am. Chem. Soc.* **1964**, *86*, 5148) and, eventually, the absolute configuration of C-3. The configuration of C-2 is always marked with a prime. See also ref 3.
(5) Van Hemelrijk, D.; Van den Enden, L.; Geise, H. J.; Sellers, H. L.; Schafer, L. *J. Am. Chem. Soc.* **1980**, *102*, 2189.
(6) Durig, J. R.; Gerson, D. J. *J. Phys. Chem.* **1981**, *85*, 426.
(7) De Haah, J. W.; Van de Ven, L. J.; Wilson, A. R. N.; Van der Hout Lodder, A. E.; Altona, C.; Faber, D. H. *Org. Magn. Reson.* **1976**, *8*, 477.
(8) The other conformations considered in this paper are obtained from the one considered in Figure 2 by rotating the C-2–C-3 bond counterclockwise with respect to the observer. H-skew = +120°; H-skew′ = +240°. H-gauche = +60°, H-anti = +180°, and H-gauche′ = +300° are not considered because of their high energy.[5–7]
(9) Bailey, W. J.; King, C. *J. Am. Chem. Soc.* **1955**, *77*, 75.
(10) Zambelli, A.; Sacchi, M. C.; Locatelli, P.; Zannoni, G. *Macromolecules* **1982**, *15*, 211.
(11) Solvay and Cie, U.K. Patent 1 391 067.
(12) Natta, G.; Morandi, M.; Crespi, G.; Moraglio, G. *Chim. Ind. (Milan)* **1957**, *39*, 275.

Macromolecules **1984**, *17*, 465–473

(13) Lindemann, L. P.; Adams, J. Q. *Anal. Chem.* **1971**, *43*, 1245.
(14) Natta, G.; Giachetti, E.; Pasquon, I.; Pajaro, G. *Chim. Ind. (Milan)* **1960**, *42*, 1091.
(15) Miyazawa, T.; Ideguchi, T. *J. Polym. Sci., Part B* **1963**, *1*, 389.
(16) Zambelli, A.; Giongo, M. G.; Natta, G. *Makromol. Chem.* **1968**, *112*, 183.
(17) Lazzaroni, R.; Salvadori, P.; Pino, P. *J. Organomet. Chem.* **1972**, *43*, 233.
(18) Ammendola, P.; Ciajolo, M. R.; Panunzi, A.; Tuzi, A. *J. Organomet. Chem.* **1983**, *254*, 389.
(19) Stefani, A.; Tatone, D.; Pino, P. *Helv. Chim. Acta* **1979**, *62*, 1098.

Studies on Stereospecific Sequence Distributions in Polypropylenes by Pyrolysis–Hydrogenation Fused-Silica Capillary Gas Chromatography

Hajime Ohtani and Shin Tsuge*

Department of Synthetic Chemistry, Faculty of Engineering, Nagoya University, Furo-cho, Chikusa-ku, Nagoya 464, Japan

Toshio Ogawa[†] and Hans-Georg Elias

Michigan Molecular Institute, Midland, Michigan 48640. *Received May 16, 1983*

ABSTRACT: The stereoregularity of various polypropylenes (PP's) has been studied by pyrolysis–hydrogenation gas chromatography with a high-resolution fused-silica capillary column. On the basis of the pyrograms obtained, average stereoregularity and stereospecific sequence length of PP's were estimated from the relative intensities among the tetramer peaks and the pentamer peaks, respecitvely. Peak intensities of the larger products were also in harmony with the estimated stereospecific sequence length. The relative peak intensities of the C_{10}-trimer peaks were used in the estimation of the degree of chemical inversion of the monomer units along the polymer chain. As a result, it was found that most of the chemical inversions were present in the syndiotactic sequences. The mechanism of the stereoisomerization accompanied by pyrolysis of PP's is also discussed.

Polypropylene (PP) is a typical stereoregular polymer, and its physical properties are affected not only by the average molecular weight and the molecular weight distribution but also by the configurational characteristics. Until now structural characterization of PP's has been carried out mainly by X-ray diffraction, IR, and NMR. The ^{13}C NMR spectra of the methyl carbons, which are clearly split corresponding to the tactic pentad placement, have been extensively applied to the determination of the stereoregularity (tacticity) of PP's in recent years.[1-4]

Pyrolysis–gas chromatography (PGC) has been also applied to the characterization of PP. Tsuchiya et al.[5] investigated the pyrolysis of isotactic PP in vacuum at around 400 °C and suggested that intramolecular transfer of secondary radicals played an important role in the degradation mechanism. Audisio et al.[6] studied stereoirregular, isotactic, and syndiotactic PP's without hydrogenation and identified some diastereoisomeric components of the tetramer fraction. The relative intensities of the diastereoisomers reflected the tacticities of the decomposed polymer. In contrast, Seeger et al.[7] made use of PGC with in-line hydrogeneation (PHGC) and achieved fairly good separation of the diastereoisomeric fragments of PP's with various tacticities. However, they pointed out that the configuration in the fragments differs from that in the original chain because of isomerization during thermal degradation and suggested that the isomerization was caused mainly by stepwise transfer of the radicals in the cyclization process. As a result of PGC with a gas density detector, Kiran et al.[8] attributed the major pyrolysis products of PP to intramolecular radical transfers in the secondary macroradicals to the 5th, 9th, and 13th carbon atoms and those in the primary macroradicals to the 6th, 10th, and 12th carbon atoms. Kiang et al.[9] and Dickens[10] investigated the kinetics and mechanism of the thermal degradation of PP's.

Recently, PHGC with a high-resolution glass capillary column has been applied to the configurational characterization of PP's.[11] The assigned characteristic peaks of tetramers (C_{11}–C_{13}) and pentamers (C_{14}–C_{16}), which reflect tactic dyads and triads, respectively, were interpreted in terms of the average stereoregularity, whereas the peaks of C_{10}-trimers were applied to the elucidation of the degree of chemical inversion of the monomer units.

In this work, the PHGC technique was modified by incorporating a fused-silica narrow-bore capillary column to obtain further improvement in the resolution of the pyrograms up to tridecamers (C_{38}–C_{40}), which reflect the longer stereospecific sequences. On the basis of the observed high-resolution pyrograms of various PP's differing in stereoregularity, the stereospecific sequence length was estimated along with the average stereoregularity. In addition, the relation between the degree of chemical inversion and stereoregularity was studied. The mechanism of the stereoisomerization accompanied by pyrolysis of PP's is also discussed in terms of intramolecular radical-transfer processes.

Experimental Section

Samples. The raw material for the predominantly isotactic PP (iso-PP) was synthesized in the presence of a typcial Ziegler–Natta catalyst, $AlEt_2Cl/TiCl_3$. PP-I(A) was prepared by removing the amorphous portions from the raw material through *n*-hexane extraction. The diethyl ether soluble fraction of the raw material was used as PP-I(B), which was expected to be mainly composed of atactic-PP (atac-PP). Predominantly syndiotactic PP (synd-PP) prepared in the presence of $AlEt_2Cl/VCl_4$ was used as PP-II. These three PP samples are the same as those used in the previous work.[11] Another raw material of PP with syndiotactic stereoblocks was synthesized in the presence of

---

[†] Present address: Hirakata Plastics Laboratory, Ube Industries Ltd., Hirakata, Osaka 573, Japan.

0024-9297/84/2217-0465$01.50/0